

**Nanofluidics of nematic liquid crystals in hollow capillaries**

Izabela Śliwa\*

*Poznan University of Economics and Business, 61-875 Poznan, Poland*Pavel V. Maslennikov<sup>†</sup>*Immanuel Kant Baltic Federal University, Kaliningrad 236040, Russia*Alex V. Zakharov<sup>‡</sup>*Saint Petersburg Institute for Machine Sciences, The Russian Academy of Sciences, Saint Petersburg 199178, Russia*

(Received 23 June 2021; accepted 6 August 2021; published 26 August 2021)

The aim of this paper is to investigate the response of a homogeneously aligned nematic nanosized hollow cavity (HANNHC) confined between two charged horizontal coaxial cylinders and subjected to both a radially applied electrostatic field  $\mathbf{E}$ , arising from the surface charge density  $\kappa$  and the temperature gradient  $\nabla T$  set between these cylinders. This was done within the framework of an extension of the classical Ericksen-Leslie theory, supplemented by thermomechanical correction of the shear stress and Rayleigh dissipation function, as well as taking into account the entropy balance equation. The physical mechanism responsible for the excitation of the hydrodynamic flow in the HANNHC is based on the interaction of the director and temperature gradients and the static electric field. Calculations show that under the influence of both the  $\nabla T$  and  $\mathbf{E}$ , a stationary flow  $u^{\text{st}}$  is excited in the HANNHC in the horizontal direction. It is shown that the electric force enforced by the flexoelectric polarization plays a crucial role in the excitation of  $u^{\text{st}}$  between these cylinders.

DOI: [10.1103/PhysRevE.104.024702](https://doi.org/10.1103/PhysRevE.104.024702)**I. INTRODUCTION**

Nanofluidics, i.e., field of nanoliter liquids physics ( $1 \text{ nl} = 10^{-12} \text{ m}^3$ ), is of great interest to researchers, because of the promising applications of these systems in biology [1], optoelectronics [2], and various sensors and actuators [3] based on anisotropic molecular liquids and liquid crystal (LC) materials. Manipulations with these nanosized anisotropic molecular systems in ultrathin capillaries and channels are often performed using an external electric field [4]. This method of transport of nanoliter volumes is equally applicable both for molecular liquids and LC materials. A distinctive feature of LC systems in comparison with anisotropic molecular liquids is that orientation ordering of molecules described by director field  $\hat{\mathbf{n}}$  is formed in LC systems under certain thermodynamic conditions [5]. It is shown that the interaction of the gradients of the director field  $\nabla \hat{\mathbf{n}}$  and the temperature  $\nabla T$  is responsible for the occurrence of a thermomechanical force, which, in turn, is responsible for the excitation of a stable hydrodynamic flow  $\mathbf{v}$  of liquid crystal materials in thin and ultrathin channels and capillaries [6]. Recently, the problem of horizontal motion in an ultrathin channel of a drop of liquid crystal, ranging in size from several tens to hundreds of nanoliters, under the influence of a temperature gradient has begun to

attract increased attention [6]. It has been shown that in the case of a hybrid aligned nematic channel, the value of the hydrodynamic flow  $\mathbf{v}$  excited by  $\nabla T$  is proportional to the tangential component of the thermomechanical stress tensor (ST)  $\sigma_{zx}^{\text{tm}}$ . In this case, the direction of hydrodynamic flow  $\mathbf{v}$  is influenced by both the direction of heat flux  $\mathbf{q}$ , caused by the temperature difference on the bounding surfaces, and the character of the preferred anchoring of  $\hat{\mathbf{n}}$  on these surfaces [6]. On the other hand, in LC channels where director anchoring on the two bounding surfaces are the same, i.e., both strongly homeotropic or homogeneous, the LC micro- or nanovolume remains quiescent under the influence of the temperature gradient. One can also consider a homogeneously aligned nematic (HAN) sample confined in a nanosized volume between two horizontal coaxial cylinders and subjected to both  $\nabla T$ , which is set between cooler inner and hotter outer cylinders, and the radially applied electrostatic field  $\mathbf{E}$ , originating from the surface charge density  $\kappa$ . In this case the micro- or nanosized HAN material settles down to a stationary flow  $u^{\text{st}}$  regime in the horizontal direction.

It should be pointed out that the pumping effect under the influence of the radially directed thermal gradient, but without electric field, is not found in the LC cavity when molecules are aligned in the same way (homeotropically or homogeneously) on both bounding surfaces.

The aim of our paper is to study the response of the HAN system confined in the nanovolume between two charged horizontal coaxial cylinders and subjected to both  $\nabla T$  and a radially applied electrostatic field  $\mathbf{E} = E(r)\hat{\mathbf{e}}_r$ , originating from the surface charge density  $\kappa$ , and hence electric double

\*izabela.sliwa@ue.poznan.pl

†pashamaslennikov@mail.ru

‡Author to whom correspondence should be addressed: alexandre.zakharov@yahoo.ca; www.ipme.ru

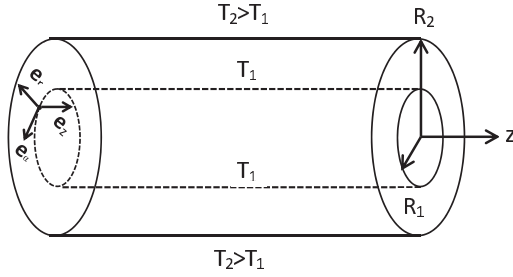


FIG. 1. The coordinate system specifying the orientation of director field  $\hat{\mathbf{n}}$ .

layers, on both boundaries. Another task is to show at what sizes of the LC cavity the influence of  $E(r)$  can be neglected.

This problem will be treated in the framework of the appropriate nonlinear extension of the classical Ericksen-Leslie theory [7,8], supplemented by the thermomechanical correction of shear stress (SS) and Rayleigh dissipation function, as well as taking into account the entropy balance equation [6,9], whereas Rayleigh-Benard mechanism does not produce any effect because of the small film thickness [10]. The present paper is organized as follows: The relevant equations describing director motion, fluid flow and temperature distribution in the above named system are given in Sec. II; numerical results for possible relaxation regime are given in Sec. III; conclusions are summarized in Sec. IV.

## II. FORMULATION OF THE RELEVANT EQUATIONS FOR NEMATIC FLUIDS

The main aim of our paper is to study the response of the HAN nanosized cavity (HANNC) composed of asymmetric polar molecules, such as *cyanobiphenyls*, at the density  $\rho$ , confined between two charged horizontal coaxial cylinders with radii  $R_1$  and  $R_2$  ( $R_2 > R_1$ ), and subjected to both  $\nabla T$ , caused by the temperature difference on the bounding cylinders, and a radially applied electrostatic field  $\mathbf{E} = E(r)\hat{\mathbf{e}}_r$ , originating from the surface charge density  $\kappa$  on these cylinders. The size of the capillary  $d$ , on a scale ranging from a few tens to hundreds of nanometers, is equal to  $R_2 - R_1$ , and these cylinders are kept at different temperatures, with the outer one  $(T_2)_{r=R_2} = T_{\text{out}}$  being hotter than the inner one  $(T_2)_{r=R_1} = T_{\text{in}}$  ( $T_2 > T_1$ ). Here  $\hat{\mathbf{e}}_r$  is the radial unit vector, directed perpendicular to the bounding cylinders, whereas the other unit vectors of the cylindrical coordinate system used here are  $\hat{\mathbf{e}}_z$ , defined by the common axis of the two cylinders, which coincides with the planar director orientations on both boundaries ( $\hat{\mathbf{e}}_z \parallel \hat{\mathbf{n}}_{r=R_1}$  and  $\hat{\mathbf{e}}_z \parallel \hat{\mathbf{n}}_{r=R_2}$ ), and the tangential one  $\hat{\mathbf{e}}_\alpha = \hat{\mathbf{e}}_z \times \hat{\mathbf{e}}_r$  (for details see Fig. 1). On assuming that both the temperature gradient  $\nabla T$ , caused by the temperature difference  $\Delta T = T_2 - T_1$  on the bounding cylinders, and the electric field  $\mathbf{E}(r)$  vary only in the  $r$  direction, we can suppose that the components of the director  $\hat{\mathbf{n}} = n_r\hat{\mathbf{e}}_r + n_z\hat{\mathbf{e}}_z = \sin\theta(r, t)\hat{\mathbf{e}}_r + \cos\theta(r, t)\hat{\mathbf{e}}_z$ , as well as the rest of the physical quantities also depend only on the coordinate  $r$  and on time  $t$ . Here  $\theta$  denotes the angle between the direction of the director  $\hat{\mathbf{n}}$  and the unit vector  $\hat{\mathbf{e}}_z$ .

It should be noted that one of the nonmechanical method for producing flow  $\mathbf{v}$  in a nanofluidic nematic channel is based

on the coupling between the temperature  $\nabla T = \frac{\partial T(r,t)}{\partial r}\hat{\mathbf{e}}_r$  and the director field  $\nabla\hat{\mathbf{n}}$  gradients [6]. Thus, a necessary condition for the excitation of the hydrodynamic flow  $\mathbf{v}$  in the HAN nanofluidic channel, under the influence of the temperature gradient, is the presence of  $\nabla\hat{\mathbf{n}}$ . In the case when the director  $\hat{\mathbf{n}}$  anchoring on two cylinders are the same, i.e., strongly homogeneous, and the electric field  $\mathbf{E}$  is not applied, then the gradient of the director field  $\hat{\mathbf{n}}$  is absent, and thus there is no deformation of the nematic cavity. There is at least one way to form  $\nabla\hat{\mathbf{n}}$  in the initially HANNC, by applying the electric field  $\mathbf{E}(r)$ , directed orthogonally to the HANNC. In our case, such a role can be played by the electric field, for instance, the electrostatic field originating from the surface charge density  $\kappa$  on both bounding surfaces, via the electric double layers [3], which can disturb the homogeneous orientation of the director field in the LC cavity confined between these cylinders, and makes the splay and bend deformations. In turn, the splay and bend elastic deformations caused by the electric field give rise to flexoelectric polarization [11]  $\mathbf{P} = e_1\hat{\mathbf{n}}(\nabla \cdot \hat{\mathbf{n}}) + e_3(\nabla \times \hat{\mathbf{n}}) \times \hat{\mathbf{n}}$ , where  $e_i$  ( $i = 1, 3$ ) denote the flexoelectric coefficients. Below, we explore a curvature of the HANNC confined between two infinitely long charged horizontal cylinders and consider the joint effect of flexoelectric polarization  $\mathbf{P}$  and the electrostatic field originating from the surface charge density  $\kappa$  on both bounding surfaces, on the director reorientation and the excitation of the hydrodynamic flow  $\mathbf{v}$  in the nanosized HAN channel. Thus, the heating  $\Delta T = T_{\text{out}} - T_{\text{in}} > 0$  of the HANNC causes the flexoelectric and thermomechanical coupling with the director's gradient  $\nabla\hat{\mathbf{n}}$ , and their correlation solve the problem of excitation of a steady flow  $\mathbf{v}$ . Here the range  $[T_{\text{out}}, T_{\text{in}}]$  falls within stability region of the nematic phase.

Notice that, in experimental term, the mesogen sample can usually contain some ions, and when the nematic is in contact with a charged solid substrate, selective ion adsorption occurs. For instance, the positive ions are attracted by the substrate, whereas the negative ones are repelled. In this case, the surface electrostatic field  $E_0$ , originating from the surface charge density  $\kappa$ , will penetrate the bulk over a distance of the order of the Debye screening length  $\lambda_D$  [12], owing to screening by the ions being present in the bulk of the LC (usually a weak electrolyte). The distance dependence of the surface electric field with bulk screening  $\lambda_D = \sqrt{\frac{\epsilon_0 k_B T}{2q^2 n_i}}$  emerges naturally from the Poisson-Boltzmann theory as [12]

$$\begin{aligned} \mathbf{E}\left(\frac{r}{\lambda_D}\right) &= E_0 E\left(\frac{r}{\lambda_D}\right)\hat{\mathbf{e}}_r \\ &= E_0 \frac{1}{\Delta} \left[ C_I \mathcal{K}_1\left(\frac{r}{\lambda_D}\right) - C_K \mathcal{I}_1\left(\frac{r}{\lambda_D}\right) \right] \hat{\mathbf{e}}_r, \end{aligned} \quad (1)$$

where  $E_0 = \kappa/(\epsilon_0\epsilon)$  is the surface electrostatic field;  $\epsilon_0$  is the absolute dielectric permittivity of free space;  $\epsilon = (\epsilon_{\parallel} + 2\epsilon_{\perp})/3$  is the isotropic dielectric constant;  $\epsilon_{\parallel}$  and  $\epsilon_{\perp}$  are the dielectric constants parallel and perpendicular to the director  $\hat{\mathbf{n}}$ , respectively;  $q$  denotes the proton charge;  $k_B$  is the Boltzmann constant; and  $n_i$  is the bulk ion concentration. Here the function  $E(r)$  is defined by  $E(r) = -\nabla\varphi$ , where  $\varphi$  has to satisfy the equation

$$\Delta\varphi(r) - \lambda_D^{-2}\varphi(r) = 0, \quad (2)$$

with the boundary conditions  $\nabla\varphi(r)_{r=R_1} = E_0\hat{e}_r$  and  $\nabla\varphi(r)_{r=R_2} = -E_0\hat{e}_r$ , respectively. Finally, the function  $\mathcal{E}(r)$  takes the form

$$E\left(\frac{r}{\lambda_D}\right) = \frac{1}{\Delta} \left[ C_I \mathcal{K}_1\left(\frac{r}{\lambda_D}\right) - C_K \mathcal{I}_1\left(\frac{r}{\lambda_D}\right) \right], \quad (3)$$

where  $\Delta = \mathcal{I}_1\left(\frac{R_2}{\lambda_D}\right)\mathcal{K}_1\left(\frac{R_1}{\lambda_D}\right) - \mathcal{I}_1\left(\frac{R_1}{\lambda_D}\right)\mathcal{K}_1\left(\frac{R_2}{\lambda_D}\right)$ ,  $C_I = \frac{1}{\Delta}[\mathcal{I}_1\left(\frac{R_1}{\lambda_D}\right) + \mathcal{I}_1\left(\frac{R_2}{\lambda_D}\right)]$ ,  $C_K = \frac{1}{\Delta}[\mathcal{K}_1\left(\frac{R_1}{\lambda_D}\right) + \mathcal{K}_1\left(\frac{R_2}{\lambda_D}\right)]$ ,  $\mathcal{I}_1$  and  $\mathcal{K}_1$  denote modified Bessel functions of the first and second kinds, respectively.

On the two delimiting cylinders, the velocity field has to satisfy the no-slip boundary condition,

$$v(r)_{r=R_1} = v(r)_{r=R_2} = 0. \quad (4)$$

Taking into account that the size of the HANNC is of a few hundreds of nanometers, one can assume the mass density  $\rho$  to be constant across the HANNC, and thus we are dealing with an incompressible fluid. The incompressibility condition  $\nabla \cdot \mathbf{v} = 0$ , coupled with the no-slip condition, implies the existence of only one nonzero component for vector  $\mathbf{v}$ , viz.,  $\mathbf{v}(r, t) = v_z(r, t)\hat{e}_z \equiv u(r, t)\hat{e}_z$ .

In the nematic phase, splay and bend deformations, caused by electric field, give rise to two independent flexoelectric coefficients ( $e_1, e_3$ ) [11]. Their contributions to the induced polarization can be written as  $\mathbf{P} = P_r\hat{e}_r + P_z\hat{e}_z$ , where the vector components are given by the classical Meyer model [11]

$$P_r = (e_1 + e_3)n_r n_{r,r} + e_1 \frac{n_r^2}{r}, \quad (5)$$

and

$$P_z = e_1 n_z \nabla_r n_r + e_3 n_r n_{z,r}, \quad (6)$$

where  $n_{i,r} = \frac{\partial n_i}{\partial r}$ , ( $i = r, z$ ) denotes the partial derivative of director components with respect to space coordinate, and  $\nabla_r(\dots) = (\dots)_{,r} + \frac{n_r}{r}$  is a divergence. Thus, the aim of this work is to study the response of a homogeneously aligned LC nanosized cavity confined between two charged horizontal coaxial cylinders and subjected to both the temperature gradient and the radially applied screening electrostatic field, created in the LC near the charged cylinders. However, the question immediately arises regarding what should be the value of the electrostatic field, originating from the surface charge density  $\kappa_{cr}$ , that is sufficient to move a small amount of nematic in the presence of the temperature gradient.

The answer to this question will be given in the framework of the classical Ericksen-Leslie theory [7,8], supplemented by the thermomechanical correction of the SS and the Rayleigh dissipation function [6], as well as the entropy balance equation [9]. The hydrodynamic equations describing the re-orientation of the HAN system in the named setting can be derived from the balance of elastic, viscous, thermomechanical, and electric torques acting on the unit LC volume, the linear momentum equation for the velocity field  $\mathbf{v}(r, t)$ , and the heat conduction equation for the temperature field  $T(r, t)$ , respectively. These equations have the form [13]

$$\left[ \frac{\delta \mathcal{W}_F}{\delta \hat{\mathbf{n}}} - \frac{\delta \psi^{el}}{\delta \hat{\mathbf{n}}} + \frac{\delta \mathcal{R}}{\delta \hat{\mathbf{n}}} \right] \times \hat{\mathbf{n}} = 0, \quad (7)$$

$$\rho \dot{\mathbf{v}} = \nabla_r \sigma + \nabla_r \psi^{el+P}, \quad (8)$$

and

$$C_p \dot{T}(r, t) = -\nabla_r q_r, \quad (9)$$

where  $2\mathcal{W}_F = K_1 n_{r,r}^2 + K_3 n_{z,r}^2$  is the elastic and  $2\psi^{el+P} = \epsilon_0 \epsilon E^2(r) + 2P_r(r)E(r)$  is the electric torque with the flexoelectric correction term, whereas  $K_1$  and  $K_3$  are the splay and bend elastic constants of the LC system, respectively. The full Rayleigh dissipation function  $\mathcal{R} = \mathcal{R}_{vis} + \mathcal{R}_{tm} + \mathcal{R}_{th}$  is composed of three contributions, which are given in the forms [13,14]  $2\mathcal{R}_{vis} = \gamma_1(\dot{n}_r^2 + \dot{n}_z^2) + u_r(\dot{n}_r n_z - \dot{n}_z n_r)[\gamma_1 + \gamma_2(n_z^2 - n_r^2)] + h(r)u_r^2$ ,  $\mathcal{R}_{tm} = \xi T_r \{ (\frac{1}{2} + n_z^2)(\dot{n}_r n_{r,r} + \dot{n}_z n_{z,r}) + \frac{1}{2r} n_r n_z (\dot{n}_z n_r - \dot{n}_r n_z) + u_r [n_{r,r}(n_z + \frac{1}{4}n_z n_r^2) - \frac{3}{4r} n_z n_r] \}$ , and  $\mathcal{R}_{th} = \frac{1}{T} T_r^2 (\lambda_{\parallel} n_r^2 + \lambda_{\perp} n_z^2)$ , corresponding to the viscous, thermomechanical, and thermal contributions, respectively. Here  $\dot{\hat{\mathbf{n}}} = \frac{d\hat{\mathbf{n}}}{dt}$  is the material derivative of the director  $\hat{\mathbf{n}}$ ,  $\rho$  is the mass density of the LC system,  $2h(r) = \alpha_4 + \frac{1}{2}(\gamma_1 + \alpha_5 + \alpha_6) + \alpha_1 n_r^2 n_z^2 + \gamma_2(n_z^2 - n_r^2)$  is the hydrodynamic function,  $\gamma_1 = \alpha_3 - \alpha_2$  and  $\gamma_2 = \alpha_3 + \alpha_2$  are the rotational viscosity coefficients of the LC system,  $\alpha_i/\alpha_6$  are the six Leslie viscosity coefficients,  $\lambda_{\parallel}$  and  $\lambda_{\perp}$  are the heat conductivity coefficient parallel and perpendicular to the director  $\hat{\mathbf{n}}$ , and  $\xi \sim 10^{-12}$  J/m K is the thermomechanical constant [6,15,16]. The full ST  $\sigma = \frac{\delta \mathcal{R}}{\delta \nabla \mathbf{v}}$  is composed of four  $\sigma = \sigma_{elast} + \sigma_{vis} + \sigma_{tm} - \mathcal{P}\mathcal{I}$  contributions, which are given in the forms  $\sigma_{elast} = -\frac{\partial \mathcal{W}_F}{\partial \nabla \hat{\mathbf{n}}} \cdot (\nabla \hat{\mathbf{n}})^T$ ,  $\sigma_{vis} = \frac{\delta \mathcal{R}_{vis}}{\delta \nabla \mathbf{v}}$ , and  $\sigma_{tm} = \frac{\delta \mathcal{R}_{tm}}{\delta \nabla \mathbf{v}}$ , corresponding to the elastic, viscous, and thermomechanical forces, whereas  $\mathcal{P}$  is the hydrostatic pressure in the HANNC and  $\mathcal{I}$  is the unit tensor, respectively.

When the gradient of temperature  $\nabla T$  is set up across the HANNC, we expect that the temperature field  $T(r, t)$  satisfies the heat conduction equation (9), where  $C_p$  is the heat capacity, and  $q_r = -T \frac{\delta \mathcal{R}}{\delta T_r}$  denotes the radial heat flux component, which in a cylindrical coordinate takes the form  $q_r = T_r (\lambda_{\parallel} n_r^2 + \lambda_{\perp} n_z^2) + \xi T [(\frac{1}{2} + n_z^2)(\dot{n}_r n_{r,r} + \dot{n}_z n_{z,r}) + \frac{1}{2r} n_r n_z (\dot{n}_z n_r - \dot{n}_r n_z)] + u_r \xi T [n_{r,r}(n_z + \frac{1}{4}n_z n_r^2) - \frac{3}{4r} n_z n_r]$ .

The Ericksen-Leslie form for the viscous part of the dissipation function gives the SS component for the geometry consideration  $\sigma_{vis} = \frac{\delta \mathcal{R}_{vis}}{\delta \nabla \mathbf{v}} = \frac{1}{2}(\dot{n}_r n_z - \dot{n}_z n_r)[\gamma_1 + \gamma_2(n_z^2 - n_r^2)] + h(r)u_r$ , whereas the thermomechanical part of dissipation function gives the corresponding contribution to SS as  $\sigma_{tm} = \frac{\delta \mathcal{R}_{tm}}{\delta \nabla \mathbf{v}} = \xi T_r [n_{r,r}(n_z + \frac{1}{4}n_z n_r^2) - \frac{3}{4r} n_z n_r]$ .

In order to observe the response of the HANNC confined between two charged horizontal coaxial cylinders and subjected both to the temperature gradient and the radially applied screening electrostatic field, we consider the dimensionless analog of the torque balance equation [see Eq. (7)]. For two component director  $\hat{\mathbf{n}} = n_r \hat{e}_r + n_z \hat{e}_z$  in a cylindrical coordinate system, the dimensionless torque balance equation reads [13]

$$\begin{aligned} n_r \dot{n}_z - n_z \dot{n}_r &= \frac{1}{2} u_{r,r} [1 - \gamma_{21}(n_z^2 - n_r^2)] \\ &\quad - E^2(r, \tau) n_r n_z - \delta_1 E(r, \tau) \mathcal{P}_z(r, \tau) \end{aligned}$$

$$\begin{aligned}
 & -\delta_2 \left\{ \frac{1}{r} [r\mathcal{K}(r)]_{,r} - (1 - K_{31})n_{z,r}^2 - \frac{1}{r^2} n_r n_z \right\} \\
 & - \frac{1}{2} \delta_3 \chi_{,r} [n_z n_{r,r} (3 + n_r^2) - n_r n_{z,r} (1 + n_r^2)],
 \end{aligned} \quad (10)$$

where  $r$  denotes the dimensionless radius (i.e., scaled by  $d$ ),  $\mathcal{K} = n_z n_{r,r} - K_{31} n_r n_{z,r}$ ,  $K_{31} = K_3/K_1$ ,  $\gamma_{21} = \gamma_2/\gamma_1$ ,  $\dot{n}_i = \frac{dn_i}{d\tau}$  ( $i = r, z$ ) is the material derivative with respect to dimensionless time  $\tau = (\epsilon_0 \epsilon E_0^2 / \gamma_1) t$ , and  $P_z(r)$  denotes the dimensionless component of the polarization vector  $\mathbf{P}$  (i.e., scaled by  $E_0 d$ ), whereas the dimensionless temperature  $\chi(r, \tau) = T(r, \tau)/T_{NI}$  is scaled by the nematic-isotropic transition value. In turn, three parameters of the LC system are as follows:  $\delta_1 = \frac{e_1}{E_0 d}$ ,  $\delta_2 = (E_{th}/\pi E_0)^2$ ,  $\delta_3 = \delta_2 \frac{\xi T_{NI}}{K_1}$ , whereas  $E_{th} = \frac{\pi}{d} \sqrt{\frac{K_1}{\epsilon_0 \epsilon_a}}$  is the critical value of the electric field  $E(r)$ .

In the case of incompressible fluid, the dimensionless Navier-Stokes equation [see Eq. (8)] reduces to [13]

$$\delta_4 u_{,r}(r, \tau) = \nabla_{,r} [\sigma_{rz}^{vis} + \sigma_{rz}^{tm}], \quad (11)$$

$$\nabla_{,r} \sigma_{rr}^{elast} - \frac{\sigma_{\alpha\alpha}^{elast}}{r} + \psi_{,r}^{el+P} = 0, \quad (12)$$

where  $\delta_4 = \frac{\rho K_1}{\gamma_1^2}$  is an extra one parameter of the LC system, whereas

$\nabla_{,r} \sigma_{rr}^{elast} = \sigma_{rr,r}^{elast} + \frac{\sigma_{rr}^{elast}}{r}$ ,  $\sigma_{rr}^{elast} = -\delta_2 [\mathcal{P}(r) + (n_{r,r} + \frac{n_r}{r}) n_{r,r} + K_{31} n_{z,r}^2]$ , and  $\sigma_{\alpha\alpha}^{elast} = -\delta_2 [\mathcal{P}(r) + (n_{r,r} + \frac{n_r}{r}) \frac{n_r}{r}]$  are two normal ST components, and  $\mathcal{P}(r)$  is the scaled hydrostatic pressure (i.e., scaled by  $K_1/d^2$ ). The Ericksen-Leslie form for the viscous and thermomechanical parts of the shear stress components for the geometry under consideration takes the forms

$$\sigma_{rz}^{vis} = \frac{1}{2} (\dot{n}_r n_z - n_r \dot{n}_z) + \gamma_{21} (n_r^2 + n_z^2) + h(r) u_{,r}, \quad (13)$$

and

$$\sigma_{rz}^{tm} = \frac{1}{4} \delta_3 \chi_{,r} [n_r n_z (1 + 2n_r^2) + 6n_z n_{r,r} - n_r^3 n_{z,r}]. \quad (14)$$

When a small mean temperature gradient (in our case  $\sim 1$  K/ $\mu$ m) is set up across the LC system, we expect the temperature field  $\chi(r, \tau)$  to satisfy the dimensionless heat conduction equation [13]

$$\delta_5 \dot{\chi} = \nabla_{,r} [\chi_{,r} (\lambda n_r^2 + n_z^2)] + \delta_6 \nabla_{,r} [\chi_{,r} \mathcal{H}(r)], \quad (15)$$

where  $\lambda = \frac{\lambda_{\perp}}{\lambda_{\parallel}}$  is the ratio of heat conductivity coefficients along and perpendicular to the director, and  $\mathcal{H}(r) = (\frac{1}{2} + n_z^2) (\dot{n}_r n_{r,r} + \dot{n}_z n_{z,r}) + \frac{1}{2r} n_z n_r (\dot{n}_z n_r - \dot{n}_r n_z) + u_{,r} [n_{r,r} (n_z + \frac{1}{4} n_z n_r^2) - \frac{3}{4r} n_z n_r]$  is the hydrodynamic function. Here  $\delta_5 = \frac{\rho C_p K_1}{\lambda_{\perp} \gamma_1}$  and  $\delta_6 = \xi \frac{K_1}{\lambda_{\perp} \gamma_1 d^2}$  are two additional parameters of the LC system.

Thus, the set of parameters involved in Eqs. (10), (11), and (15) is  $\delta_1 = \frac{e_1}{E_0 d}$ ,  $\delta_2 = (E_{th}/\pi E_0)^2$ ,  $\delta_3 = \delta_2 \frac{\xi T_{NI}}{K_1}$ ,  $\delta_4 = \frac{\rho K_1}{\gamma_1^2}$ ,  $\delta_5 = \frac{\rho C_p K_1}{\lambda_{\perp} \gamma_1}$ , and  $\delta_6 = \xi \frac{K_1}{\lambda_{\perp} \gamma_1 d^2}$ .

We will assume the homogeneous strong anchoring of the director on both bounding cylinders, i.e.,

$$(n_r)_{r=r_1} = (n_r)_{r=r_2} = 0, \quad (16)$$

together with the no-slip conditions

$$u(r)_{r=r_1} = u(r)_{r=r_2} = 0, \quad (17)$$

where we used the corresponding dimensionless radii  $r_i = R_i/d$  ( $i = 1, 2$ ). The boundary conditions on dimensionless temperature are reduced to

$$\chi(r)_{r=r_1} = \chi_1, \chi(r)_{r=r_2} = \chi_2, \quad (18)$$

where the dimensionless temperature  $\chi = T/T_{NI}$  is scaled by the nematic-isotropic transition value.

As the next step we choose the surface charge density  $\kappa$  corresponding to the experimentally obtained values. The condition for production the distortion of nematic nanocavity is  $\kappa > \kappa_{cr}$ , which inputs the electric field component  $E(r)$  self-consistently with the nematic distortion of  $\hat{\mathbf{n}}$ . Taking into account that the value of the surface charge density  $\kappa$  can be expressed as  $\kappa = q n_s$ , where  $q = 1.6 \times 10^{-19}$  C is the proton charge and  $n_s$  denotes the surface ion concentration, which is varied between  $10^{15}$  and  $10^{17}$  m $^{-2}$  [17], our choice of  $n_s \approx 2.5 \times 10^{16}$  m $^{-2}$  seems reasonable. Thus, in this case  $\kappa$  is equal to  $4 \times 10^{-3}$  C/m $^2$ .

For the case of 4-*n*-pentyl-4'-cyanobiphenyl (5CB), at the temperature  $T_{in} = 300$  K and density  $10^3$  kg/m $^3$ , the experimental data for elastic constants are  $K_1 = 10.5$  pN and  $K_3 = 13.8$  pN [18], whereas the measured data for the dielectric constants are  $\epsilon_{\parallel} = 18$  and  $\epsilon_{\perp} = 8$  [19], as well as the measured  $\gamma_1 \sim 0.072$  Pa s and  $\gamma_2 \sim -0.079$  Pa s [20]. At the temperature of 300 K and density of  $10^3$  kg/m $^3$ , values of the six Leslie coefficients (in Pa s) were found to be [20]  $\alpha_1 \sim -0.0066$ ,  $\alpha_2 \sim -0.075$ ,  $\alpha_3 \sim -0.0035$ ,  $\alpha_4 \sim 0.072$ ,  $\alpha_5 \sim 0.048$ , and  $\alpha_6 \sim -0.03$ , respectively. The value of the heat capacity  $C_p$  is equal to  $10^3$  J/kg K [21], whereas the value of the thermal conductivity coefficients are [22]  $\lambda_{\parallel} = 0.24$  W/m K and  $\lambda_{\perp} = 0.13$  W/m K, respectively. The magnitude of the Debye length depends solely on the properties of the LC and not on any property of the surface. In the case of homogeneous alignment of the 5CB layers on both cylinders, and  $n_{eq} \sim 5 \times 10^{20}$  m $^{-3}$  [17], the Debye length is equal to  $\lambda_D \sim 50$  nm.

Two parameters of our system of the nonlinear partial differential equations (10), (11), and (15),  $\delta_1 = (\frac{E_{th}}{\pi E_0})^2$  and  $\delta_2 = \xi \frac{T_{NI}}{K_1} \delta_1$ , include the value of the threshold electric field  $E_{th} = \frac{\pi}{d} \sqrt{\frac{K_1}{\epsilon_0 \epsilon_a}}$ , which is inversely proportional to the thickness  $d$  of the HANNC. Thus, we have a set of parameters corresponding to different cavity thicknesses:  $D = d/\lambda_D = 2.0, 4.0, 8.0$ , and  $16.0$ , respectively. For the case of 5CB, at the temperature corresponding to nematic phase, the set of values of the threshold electric field are as follows:  $E_{th}(D = 2.0) = 1.15 \times 10^{-3}$ ,  $E_{th}(D = 4.0) = 0.59 \times 10^{-3}$ ,  $E_{th}(D = 8.0) = 0.30 \times 10^{-3}$ , and  $E_{th}(D = 16.0) = 0.15 \times 10^{-3}$ , respectively, calculated in units C/m $^2$ . In turn, the set of  $\delta_1$  are as follows:  $\delta_1(D = 2.0) \sim 9.0 \times 10^{-4}$ ,  $\delta_1(D = 4.0) \sim 2.5 \times 10^{-4}$ ,  $\delta_1(D = 8.0) \sim 6.0 \times 10^{-5}$ , and  $\delta_1(D = 16.0) \sim 1.5 \times 10^{-5}$ , whereas the set of  $\delta_2$  are as follows:  $\delta_2(D = 2.0) \sim 2.6 \times 10^{-2}$ ,  $\delta_2(D = 4.0) \sim 7.3 \times 10^{-3}$ ,  $\delta_2(D = 8.0) \sim 1.75 \times 10^{-3}$ , and  $\delta_2(D = 16.0) \sim 4.4 \times 10^{-4}$ , respectively. The other parameters  $\delta_3, \delta_4, \delta_5$ , and  $\delta_6$  do not depend on the cavity thickness  $d$  and are equal to  $\delta_3 \sim 0.016$ ,  $\delta_4 \sim 9 \times 10^{-4}$ ,  $\delta_5 \sim 2 \times 10^{-3}$ , and  $\delta_6 \sim 7.0 \times 10^{-7}$ . For example, the values of parameters  $\delta_1(D =$



2.0) and  $\delta_2(D = 2.0)$  are approximately 60 times greater than the values of parameters  $\delta_1(D = 16.0)$  and  $\delta_2(D = 16.0)$ .

Subsequent calculations will show how the changes in the values of parameters  $\delta_i$  ( $i = 1, 2$ ), included in the system of the nonlinear partial differential equations (10), (11), and (15), will affect the nature of the hydrodynamic flow  $\mathbf{v}$ , excited both by the temperature difference  $\Delta\chi = \chi_{\text{out}} - \chi_{\text{in}}$  and the surface electric field  $\mathbf{E}$ , originating from the surface charge density  $\kappa$ .

Using the fact that  $\delta_4 \ll 1$ , the Navier-Stokes equation (11) can be considerably simplified as the velocity follows adiabatically the motion of the director. Thus, the whole left-hand side of Eq. (11) can be neglected, so that the equation takes the form

$$\sigma_{rz}^{\text{vis}} + \sigma_{rz}^{\text{tm}} = \frac{\mathcal{C}(\tau)}{r}, \quad (19)$$

where  $\mathcal{C}(\tau)$  is a function that does not depend on  $r$  and will be fixed by the boundary no-slip conditions [see Eq. (17)]. In turn, using the fact that  $\delta_5$  and  $\delta_6 \ll 1$ , the heat conduction equation (15) can be reduced to

$$\nabla_{,r}[\chi_{,r}(\lambda n_r^2 + n_z^2)] = 0, \quad (20)$$

which has a solution

$$\chi(r, \tau) = \frac{\Delta\chi}{\mathcal{I}} \int_{r_1}^r \frac{dr}{r(\lambda n_r^2 + n_z^2)} + \chi_1, \quad (21)$$

where  $\Delta\chi = \chi_2 - \chi_1$ , and the function  $\mathcal{I}(\tau)$  is equal to  $\int_{r_1}^{r_2} \frac{dr}{r(\lambda n_r^2 + n_z^2)}$ . The smallest initial perturbation of the director component  $n_r(r, \tau_0)$  gives the initial values  $\mathcal{I}(\tau_0)$ , defined by the boundary conditions Eq. (18). In the case of the cylindrical geometry, the balance of linear momentum Eq. (12) can be used here for defining the pressure  $\mathcal{P}(r)$ , and has the solution

$$\mathcal{P}(r, \tau) = \psi^{\text{el}+P} + \sigma_{rr}^{\text{elast}} + \int_{r_1}^r \frac{\sigma_{rr}^{\text{elast}} - \sigma_{\alpha\alpha}^{\text{elast}}}{r} dr + \mathcal{P}_0, \quad (22)$$

where  $\mathcal{P}_0$  is an arbitrary constant. As for numerical solution of the above equations (10), (11), and (15), the director rotation rate is eliminated from the system of equations by means of Eqs. (10) and (11), and the value of  $\mathcal{C}(\tau_0)$  can be found using the boundary conditions [Eqs. (16) and (17)]. The initial velocity gradient  $u_r(r, \tau_0)$  from Eqs. (19)–(21) yields the new director component distribution  $n_r(r, \tau_0 + \Delta\tau)$  from Eq. (10), and the procedure is iterated up to the stationary state of  $n_r^{\text{st}}(r)$ , which imposes the stationary distributions of velocity  $u^{\text{st}}(r)$  and temperature  $\chi^{\text{st}}(r)$ . The thermodynamic condition:  $\mathcal{R}_{\text{full}} < 0$ ,  $\mathcal{R}_{\text{full}} = \int_{r_1}^{r_2} \mathcal{R} dr$  [23] yields a check on convergence.

### III. NUMERICAL RESULTS

Now we will focus on the numerical study of the effect of both the temperature  $\nabla\chi$  and the director field  $\nabla\hat{\mathbf{n}}$  gradients on the process of excitation of the hydrodynamic flow  $\mathbf{v}$  in the HANNC of thickness  $d$ . In our case  $\nabla\chi$  is produced by the temperature difference  $\Delta\chi = \chi_2 - \chi_1 = 0.0162$  ( $\sim 7$  K), which is set between cooler inner [ $\chi_{r=r_1} = \chi_1 = 0.97$  ( $\sim 300$  K)] and hotter outer [ $\chi_{r=r_2} = \chi_2 = 0.9862$  ( $\sim 307$  K)]

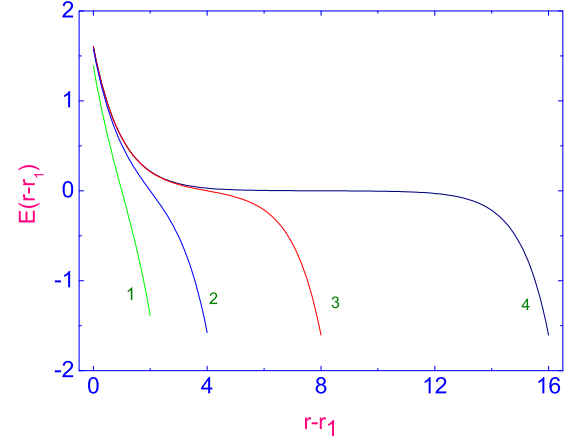


FIG. 2. Distance dependence  $r - r_1$  of the electrostatic field  $E(r - r_1)$ , calculated using Eq. (3). As explained in the text, four values of the dimensionless cavity thickness  $D = d/\lambda_D = 2.0$  (curve 1), 4.0 (curve 2), 8.0 (curve 3), and 16.0 (curve 4), have been used throughout.

cylinders, whereas  $\nabla\hat{\mathbf{n}}$ , in the initially homogeneously aligned nanofluidic cavity, is set up due to accounting the surface electric field  $E_0$ . Taking into account that the surface electric field penetrates the bulk of the LC phase on the order of the Debye screening length  $\lambda_D$  from both cylinders, the ratio  $\lambda_D/d$  will significantly affect the nature of the hydrodynamic flow in the nanofluidic cavity.

First of all, Fig. 2 shows the distribution of the electrostatic field  $E(r - r_1)$ , produced by the surface charge density  $\kappa$  on both bounding surfaces, and calculated using Eq. (3), for the four values of the dimensionless cavity thickness  $D = d/\lambda_D = 2.0$  (curve 1), 4.0 (curve 2), 8.0 (curve 3), and 16.0 (curve 4), respectively.

According to our calculations, the ranges of distance  $r$ , counted from the inner cylinder ( $r = r_1$ ), over which the charged surfaces cannot perturb the nematic phase there is only in the case of  $D = d/\lambda_D = 16.0$  [see Fig. 2 (curve 4)] and is equal to  $r_1 + 4.0 \leq r \leq r_1 + 12.0$ . In other words, with the fixed distance  $d = 16.0\lambda_D$  ( $\sim 0.8$   $\mu\text{m}$ ) between two boundaries, the influence of the electrostatic field  $E_0$ , produced by the surface charge density  $\kappa = 4.0 \times 10^{-3}$  C/m<sup>2</sup>, is restricted to the boundary layers  $r_1 \leq r \leq r_1 + 4.0$  and  $r_1 + 12.0 \leq r \leq r_1 + 16.0$ , and its role becomes negligible in the above central region.

In this study we investigate the joint effect of flexoelectric polarization  $\mathbf{P}$  and thermomechanical force, caused by the coupling of two gradients,  $\nabla\chi$  and  $\nabla\hat{\mathbf{n}}$ , on the orientational dynamics of the HANNC cavity confined between two charged cylinders and subjected to the temperature gradient, caused by the temperature difference on these cylinders. Each calculation will be repeated both for the case involving no flexoelectric polarization, defined by setting  $\mathbf{P} = 0$  [see the curves shown in Figs. 3(a) to 4(a)], as well as for the case with accounting the flexoelectric polarization  $\mathbf{P} \neq 0$  [see the curves shown in Figs. 3(b) to 4(b)] throughout the relevant equations. Calculations for both models use the relaxation criterion  $\epsilon = |[n_r(r, \tau_{m+1}) - n_r(r, \tau_m)]/n_r(r, \tau_m)|$  with  $\epsilon = 10^{-4}$ , and the

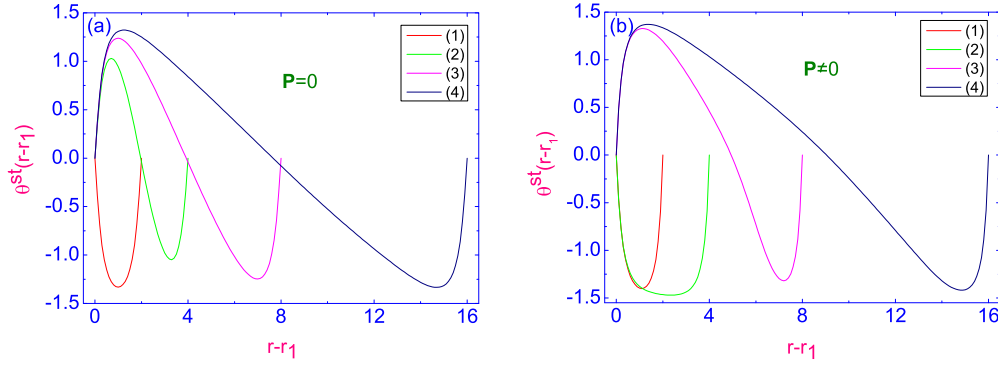


FIG. 3. Plot of the stationary radial distribution of the polar angle  $\theta^{\text{st}}(r - r_1)$  across the dimensionless HAN cavity  $r_1 \leq r \leq r_2$ , under the effect of the electric field  $E_0$ , caused by the surface density  $\kappa = 4 \times 10^{-3} \text{ C/m}^2$ , and the temperature difference  $\Delta\chi = 0.0162$ , both for the cases of  $\mathbf{P} = 0$  (a) and  $\mathbf{P} \neq 0$  (b), respectively. As explained in the text, four values of the dimensionless cavity thickness  $D = d/\lambda_D = 2.0$  (curve 1), 4.0 (curve 2), 8.0 (curve 3), and 16.0 (curve 4), have been used throughout.

numerical procedure was then carried out until a prescribed accuracy was achieved. Here  $m$  denotes the iteration number.

The relaxation processes of the radial director component  $n_r(r, \tau)$ , described by the angle  $\theta(r, \tau)$ , the velocity  $u(r, \tau)$ , and the temperature field  $\chi(r, \tau)$  across the dimensionless HAN cavity has been obtained by solving the system of nonlinear partial differential equations (10), (19), and (21), together with the boundary conditions Eqs. (16)–(18), and the initial condition  $n_r(r, \tau = 0) = 0.001$  ( $r_1 < r < r_2$ ), by means of the numerical relaxation method [24]. In our calculations, we have been using four values of the dimensionless cavity thickness  $D = d/\lambda_D = 2.0$  ( $\sim 0.1 \mu\text{m}$ ),  $4.0$  ( $\sim 0.2 \mu\text{m}$ ),  $8.0$  ( $\sim 0.4 \mu\text{m}$ ), and  $16.0$  ( $\sim 0.8 \mu\text{m}$ ), the surface charge density  $\kappa = 4.0 \times 10^{-3} \text{ C/m}^2$ , and the heating regime with the temperature difference  $\Delta\chi = \chi_2 - \chi_1 = 0.9862 - 0.97 = 0.0162$  ( $\sim 7 \text{ K}$ ), respectively. Figure 3 shows the response of the dimensionless HAN cavity confined between two horizontal coaxial cylinders and subjected to both the temperature gradient  $\nabla\chi$ , which is set up between cooler inner and hotter outer cylinders, and the electrostatic field  $E_0$ , produced by the surface charge density  $\kappa$  on both bounding cylinders, in the form of the stationary profile of the radial component of

the director  $n_r$ , which in our case is described by the distribution of the stationary polar angle  $\theta^{\text{st}}(r - r_1)$  across the entire cavity. This stationary radial distribution of the polar angle  $\theta^{\text{st}}(r - r_1)$  is the result of the relaxation of the polar angle  $\lim_{\tau \rightarrow \tau_R} \theta(r - r_1, \tau) = \theta^{\text{st}}(r - r_1)$  across the dimensionless HAN cavity  $r_1 \leq r \leq r_2$  [ $r_2 = r_1 + D(i)$ ], with the different thicknesses  $D(i) = d/\lambda_D = i$  ( $i = 2, 4, 8, 16$ ), under the effect of the electrostatic field  $E_0$ , produced by the surface charge density  $\kappa = 4 \times 10^{-3} \text{ C/m}^2$ , and the heating regime with the temperature difference  $\Delta\chi = 0.0162$  ( $\sim 7 \text{ K}$ ). The results of calculations are shown both for the cases of  $\mathbf{P} = 0$  [see Fig. 3(a)] and  $\mathbf{P} \neq 0$  [see Fig. 3(b)], respectively.

Calculations have shown that the distribution of the stationary angle  $\theta^{\text{st}}(r - r_1)$  across the dimensionless HAN cavity, under the action of the electrostatic field  $E(r)$ , calculated using Eqs. (10), (19), and (21), is weakly affected by flexoelectric polarization  $\mathbf{P} \neq 0$  only in the case of an ultrathin cavity with  $D(2) = 2.0$  ( $\sim 0.1 \mu\text{m}$ ) [see curves 1, on the Figs. 3(a) and 3(b), respectively]. With an increase in the thickness of the HAN cavity with  $D(2) = 2.0$  ( $\sim 0.1 \mu\text{m}$ ) up to  $D(4) = 4.0$  ( $\sim 0.2 \mu\text{m}$ ) and thicker, taking into account the flexoelectric polarization leads to a qualitative change in

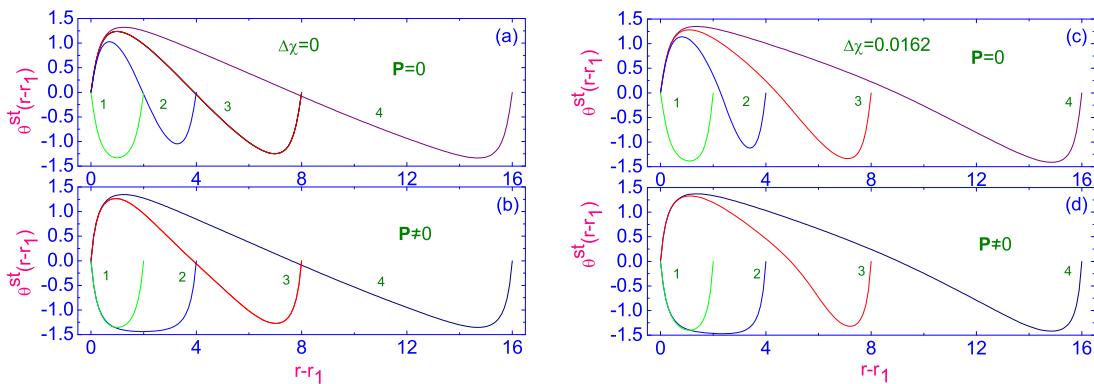


FIG. 4. Plot of the stationary radial distribution of the polar angle  $\theta^{\text{st}}(r - r_1)$  across the dimensionless HAN cavity  $r_1 \leq r \leq r_2$ , under the effect of the electric field  $E_0$ , caused by the surface density  $\kappa = 4 \times 10^{-3} \text{ C/m}^2$ , both for the cases of  $\mathbf{P} = 0$  (a) and  $\mathbf{P} \neq 0$  (b), respectively. Here the temperature difference  $\Delta\chi$  is equal to 0. [(c) and (d)] Same as described in the cases (a) and (b), but with accounting the temperature difference  $\Delta\chi = 0.0162$ . As explained in the text, four values of the dimensionless cavity thickness  $D = d/\lambda_D = 2.0$  (curve 1), 4.0 (curve 2), 8.0 (curve 3), and 16.0 (curve 4), have been used throughout.

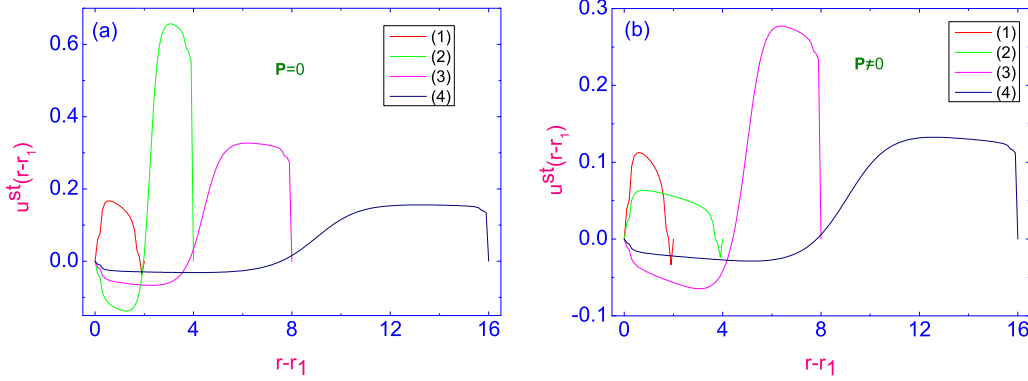


FIG. 5. Same as described in the caption of Fig. 3, but a plot of the stationary radial distribution of the velocity component  $u^{\text{st}}(r - r_1)$  across the dimensionless HAN cavity  $r_1 \leq r \leq r_2$ .

the nature of the orientation dynamics. Figures 3(a) and 3(b) (curves 2, 3, and 4) show the most pronounced effect of the flexoelectric polarization  $\mathbf{P} \neq 0$  on the stationary profile of the radial component of the director  $n_r$ , which in our case is described by the distribution of the stationary polar angle  $\theta^{\text{st}}(r - r_1)$ . So, in the case of  $\mathbf{P} = 0$ , the viscous  $T_{\text{vis}}$ , elastic  $T_{\text{elast}}$ , thermomechanical  $T_{\text{tm}}$ , and electric  $T_{\text{el}}$  torques acting on the unit LC volume produce the complex reorientation of the radial director component  $n_r$  [curves from 2 to 4 in Fig. 3(a)], which is finally described by the distribution of the stationary angle  $\theta^{\text{st}}(r - r_1)$ , across the entire cavity. This process shows that the electric torque near the inner cylinder  $r = r_1$  perturbs the radial director component in positive sense and in opposite sense near the outer cylinder  $r = r_1 + D(i)$ , ( $i = 4, 8, 16$ ). The values of  $n_r$  have become positive and the convex profile for reorientation is building up [Fig. 3(a), curves 2, 3, and 4], over the intervals  $0 \leq r \leq 2.0$ , for the case of  $D(4) = 4.0$ ,  $0 \leq r \leq 4.0$ , for the case of  $D(8) = 8.0$ , and  $0 \leq r \leq 8.0$ , for the case of  $D(16) = 16.0$ , respectively. In turn, the electric torque near the outer cylinder  $r = r_2$  perturbs the radial director component  $n_r$  in negative sense, and the values of  $n_r$  have become negative and the concave profile for reorientation is building up [Fig. 3(a), curves 2, 3, and 4], over the intervals  $2.0 \leq r \leq 4.0$ , for the case of  $D(4) = 4.0$ ,  $4.0 \leq r \leq 8.0$ , for the case of  $D(8) = 8.0$ , and  $8.0 \leq r \leq 16.0$ , for the case of  $D(16) = 16.0$ , respectively. At the same time, these profiles are antisymmetric with respect to the middle of the HAN cavity. In turn, the flexoelectric polarization  $\mathbf{P} \neq 0$  leads to a change in the nature of the orientation dynamics for the case of  $D(4) = 4.0$  ( $\sim 0.2 \mu\text{m}$ ), whereas in the case of thicker HAN cavities, such as  $D(8) = 8.0$  ( $\sim 0.4 \mu\text{m}$ ) and  $D(16) = 16.0$  ( $\sim 0.8 \mu\text{m}$ ), the orientation dynamics remains qualitatively the same, with the exception that the profiles are no longer antisymmetric with respect to the middle of the cavities [see curves 3 and 4, on the Figs. 3(a) and 3(b), respectively], and slightly shifted toward the outer cylinder. Thus, in the case of thicker cavities, such as  $D(8) = 8.0$  ( $\sim 0.4 \mu\text{m}$ ) and  $D(16) = 16.0$  ( $\sim 0.8 \mu\text{m}$ ), the consideration of flexoelectric polarization  $\mathbf{P} \neq 0$  leads to a shift of the profiles of the stationary angle  $\theta^{\text{st}}(r - r_1)$  across the entire cavity toward the outer cylinder, and these Figs. 3(a) and 3(b) show the most pronounced effect both of the dimensionless thickness  $D$  and the flexoelectric polarization

$\mathbf{P} \neq 0$  on the orientational dynamics in the dimensionless HAN cavity.

The curves shown in Figs. 4(a) correspond to the stationary radial distribution of the polar angle  $\theta^{\text{st}}(r - r_1)$  across the dimensionless HAN cavity  $r_1 \leq r \leq r_2$ , under the effect of the electric field  $E_0$ , caused by the surface density  $\kappa = 4 \times 10^{-3} \text{ C/m}^2$ , both for the cases of  $\mathbf{P} = 0$  (a) and  $\mathbf{P} \neq 0$  (b), respectively. Here the temperature difference  $\Delta\chi$  is equal to 0. In turn, the curves shown in Figs. 4(b) correspond to the stationary radial distribution of the polar angle  $\theta^{\text{st}}(r - r_1)$  across the dimensionless HAN cavity  $r_1 \leq r \leq r_2$ , under the effect of the electric field  $E_0$ , caused by the surface density  $\kappa = 4 \times 10^{-3} \text{ C/m}^2$ , and the temperature difference  $\Delta\chi = 0.0162$  ( $\sim 7 \text{ K}$ ), both for the cases of  $\mathbf{P} = 0$  (a) and  $\mathbf{P} \neq 0$  (b), respectively. The results of the comparison of these two scenarios, with and without accounting the effect of the temperature gradient, indicate that the influence of  $\nabla\chi$  is insignificant on the process of reorientation of the radial component  $n_r(r)$  of the director field.

The curves shown in Figs. 5(a) and 5(b) correspond to the stationary radial distribution of the dimensionless velocity component  $u^{\text{st}}(r - r_1)$  across the dimensionless HAN cavity confined between two horizontal coaxial cylinders, and subjected to both the temperature gradient  $\nabla\chi$ , which is set up between cooler inner and hotter outer cylinders, and the electrostatic field  $E_0$ , produced by the surface charge density  $\kappa$  on both bounding cylinders. The curves shown in Figs. 5(a) correspond to the case involving no flexoelectric polarization, defined by setting  $\mathbf{P} = 0$ , whereas the curves shown in Figs. 5(b) correspond to the case with accounting the flexoelectric polarization  $\mathbf{P} \neq 0$  throughout the relevant equations.

Calculations have shown that, following changes in the distribution of the stationary profile of the radial component of the director  $n_r$ , the distribution of the stationary radial component of the velocity  $u^{\text{st}}(r - r_1)$  across the dimensionless HAN cavity  $r_1 \leq r \leq r_2$  is strongly influenced by flexoelectric polarization  $\mathbf{P} \neq 0$ . Indeed, in the case of an ultrathin cavity with the dimensionless thickness  $D = d/\lambda_D = 2.0$  ( $\sim 0.1 \mu\text{m}$ ), both profiles of the velocity  $u^{\text{st}}(r - r_1)$  across the dimensionless HAN cavity  $r_1 \leq r \leq r_2$ , for the cases of  $\mathbf{P} = 0$  [see Fig. 5(a), curve 1] and  $\mathbf{P} \neq 0$  [see Fig. 5(b), curve 1], are characterized by qualitatively similar convex profiles through-

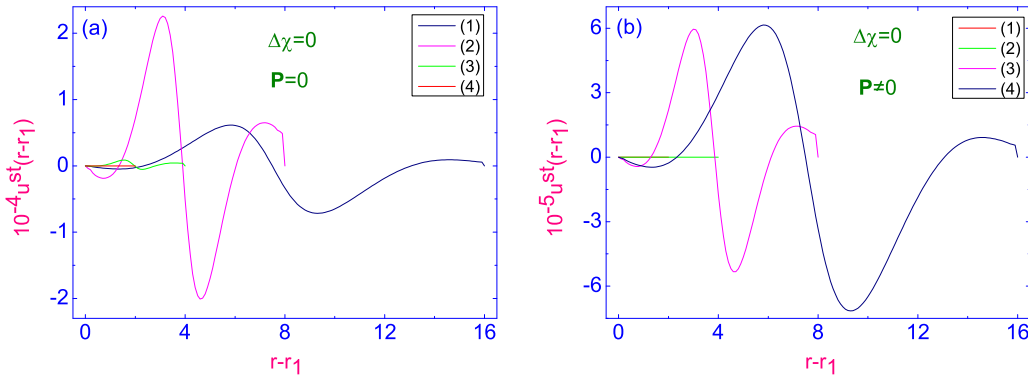


FIG. 6. Plot of the stationary radial distribution of the velocity component  $u^{\text{st}}(r - r_1)$  across the dimensionless HAN cavity  $r_1 \leq r \leq r_2$ , under the effect of the electric field  $E_0$ , caused by the surface density  $\kappa = 4 \times 10^{-3} \text{ C/m}^2$ , both for the cases of  $\mathbf{P} = 0$  (a) and  $\mathbf{P} \neq 0$  (b), respectively. Here the temperature difference  $\Delta\chi = 0.0$ . As explained in the text, four values of the dimensionless cavity thickness  $D = d/\lambda_D = 2.0$  (curve 1), 4.0 (curve 2), 8.0 (curve 3), and 16.0 (curve 4), have been used throughout.

out the cavity. In the case of  $\mathbf{P} = 0$ , the entire volume of the liquid crystal, excluding a small area near the outer cylinder, moves in the positive direction almost twice as fast as in the case of  $\mathbf{P} \neq 0$ . With a doubling of the cavity, a qualitative change in the velocity profile occurs. In the case of  $\mathbf{P} = 0$ , half of the volume of the LC cavity in the vicinity to the inner cylinder moves in the negative direction, while the other part of the HAN cavity in the vicinity to the outer cylinder moves in the positive direction [see Fig. 5(a), curve 2], whereas in the case of  $\mathbf{P} \neq 0$ , the entire volume of the HAN cavity, with the exception of a small area near the outer cylinder, moves in the positive direction almost twice as slowly as in the case of the ultrathin [ $D(2)$ ] cavity. At the same time the maximum stationary velocity [ $u_{\text{max}}^{\text{st}}(r = 3.09) = 0.65$ ] in the case of  $\mathbf{P} = 0$  is approximately 10 times greater than in the case of  $\mathbf{P} \neq 0$ . Thus, accounting the flexoelectric polarization  $\mathbf{P}$  leads to the slowing of the hydrodynamic flow in the dimensionless HAN cavity, under the effect of both the electrostatic field  $E_0$  and  $\nabla\chi$ .

With the further increase in the size of the cavity, from  $D(4) = 4.0$  ( $\sim 0.2 \mu\text{m}$ ) to  $D(8) = 8.0$  ( $\sim 0.4 \mu\text{m}$ ) and  $D(16) = 16.0$  ( $\sim 0.8 \mu\text{m}$ ), the stationary velocity profiles  $u^{\text{st}}(r - r_1)$  across the dimensionless HAN cavity  $r_1 \leq r \leq r_2$  corresponding to the cases of  $\mathbf{P} = 0$  and  $\mathbf{P} \neq 0$  become qualitatively similar to each other. In this case, part of the volume of the HAN cavity in the vicinity to the inner cylinder moves in the negative direction, while the other part of the HAN cavity in the vicinity to the outer cylinder moves in the positive direction. At the same time, the maximum of the stationary velocity  $u_{\text{max}}^{\text{st}}$ , for both dimensionless sizes  $D(8)$  and  $D(16)$ , in the positive direction is approximately 4.5 times faster than in the negative direction, whereas accounting the flexoelectric polarization  $\mathbf{P} \neq 0$  leads to a slowdown in the flow in the HAN cavity.

The curves shown in Figs. 6(a) and 6(b) correspond to the stationary radial distribution of the dimensionless velocity component  $u^{\text{st}}(r - r_1)$  across the dimensionless HAN cavity confined between two horizontal coaxial cylinders, and subjected to the electrostatic field  $E_0$ , produced by the surface charge density  $\kappa$  on both bounding cylinders. Here the temperature difference  $\Delta\chi$  is equal to 0. The results of the comparison of these two scenarios, with [see Figs. 5(a) and

5(b)] and without [see Figs. 6(a) and 6(b)] accounting the effect of the temperature gradient, indicate that the influence of  $\nabla\chi$  on the process of formation of the stationary flow  $u^{\text{st}}(r - r_1)$  in the HAN cavity confined between two horizontal coaxial cylinders and subjected to the electrostatic field  $E_0$ , produced by the surface charge density  $\kappa$  on both bounding cylinders, is significant. The influence of the electrostatic field  $E_0$  on the formation of the hydrodynamic flow  $u^{\text{st}}(r - r_1)$  in the dimensionless HAN cavity is so negligible in comparison with the influence of  $\nabla\chi$  that it can be completely ignored.

It should also be noted that in the case of ultrathin HAN cavities, with  $D(i)$ , ( $i = 2, 4$ ), the electrostatic field  $E_0$ , produced by the surface charge density  $\kappa$  on both bounding cylinders and directed across the LC cavity, completely blocks the flow  $u^{\text{st}}(r - r_1)$  of the LC material [see Fig. 6(b), curves 1 and 2]. In this case, the contribution of the electric force prevails over the contribution of viscous and elastic forces and any horizontal steady flow of the LC phase stops in the HANNC, since under the influence of electrostatic field the dipoles of molecules forming the LC phase are oriented along this field. This once again shows that the macroscopic description of the nature of the hydrodynamic flow of an anisotropic fluid subtly senses the microscopic structure of the LC material.

In the case of nano- or microfluidic LC channels, the main factor influencing the formation of the hydrodynamic flow is the external electric field, whether it is an electrostatic field or due to a voltage applied between two coaxial cylinders [25].

#### IV. CONCLUSION

In summary, we have investigated the response of the HANNC composed of asymmetric polar molecules, such as *cyanobiphenyls*, confined between two charged horizontal coaxial cylinders and subjected to both the temperature gradient and the radially applied screening electrostatic field. These cylinders were kept at different temperatures  $\Delta T = T_{\text{out}} - T_{\text{in}}$ , with the outer one being hotter than the inner cooler one and subjected to the radially applied electrostatic field  $E_0$ , caused by the surface charge density  $\kappa$  on these bounding cylinders. In this case the electrostatic field  $E_0$ , applied across the HANNC, disturbs the homogeneous orientation of the



director field in the LC cavity with thickness  $d$  and makes the splay and bend deformations. In the nematic phase, these deformations induced flexoelectric polarization  $\mathbf{P}$ , which enforced the electric torque acting per unit LC volume. In this study we investigate the joint effect of flexoelectric polarization  $\mathbf{P}$  and thermomechanical force, caused by the coupling of the temperature and the director field gradients on the process of excitation of the hydrodynamic flow  $\mathbf{v}$  in the HAN nanosized cavity.

In our case, the temperature gradient  $\nabla T$  is formed due to the temperature difference  $\Delta T = T_{\text{out}} - T_{\text{in}}$  on both bounding cylinders, which must fall within the nematic stability range. Our calculations, based on the appropriate nonlinear extension of the classical Ericksen-Leslie theory, supplemented by the thermomechanical correction of the shear stress and the Rayleigh dissipation function, as well as the entropy balance equation, show that under the influence of both the radially applied electrostatic field  $E_0$ , caused by the surface charge density  $\kappa$  on both bounding cylinders, and the heating regime  $\Delta T = T_{\text{out}} - T_{\text{in}}$ , the stationary flow  $\mathbf{v} = u^{\text{st}}(r)\hat{\mathbf{e}}_z$ , directed parallel to the bounding cylinders, is set up. It is shown that the electric force enforced by the flexoelectric polarization plays a crucial role in the formation of the horizontal flow between these cylinders. Taking into account that the surface electric field penetrates the bulk of the LC phase on the order of the Debye screening length  $\lambda_D$  from both cylinders, the ratio  $\lambda_D/d$  significantly affects the nature of the hydrodynamic flow in the nanofluidic cavity. Thus, our calculations show that the most pronounced effect of flexoelectricity in the HAN nanosized cavity between two coaxial cylinders is observed on the flow velocity and the effect on the orientational dynamics is weak.

It is also shown that in LC cavities starting from the size of 1 micron or more, the influence of the electrostatic field, originated from the surface charge density on both bounding surfaces can be neglected.

The effect of both the electrostatic field  $E_0$ , caused by the surface charge density  $\kappa = 4.0 \times 10^{-3} \text{ C/m}^2$ , and the heating regime  $\Delta T \sim 7 \text{ K}$  on the stationary flow  $\mathbf{v}^{\text{st}}(r) = u^{\text{st}}(r)\hat{\mathbf{e}}_z$ , directed parallel to the bounding cylinders, probably can be observed in the HAN cavity. The temperature difference  $\Delta T = T_{\text{out}} - T_{\text{in}} \sim 7 \text{ K}$ , for the experimentally well studied and technologically interesting case of 4-*n*-pentyl-4'-cyanobiphenyl (5CB), can be achieved by pumping the cooling material (with a temperature  $T_{\text{in}}$  less than with 7 degrees below room temperature  $T_{\text{out}}$ ) through the inner cylinder. At such conditions, in the HAN microcavity with the thickness  $d \sim 0.4 \mu\text{m}$ , the maximal stationary velocity  $u^{\text{st}}(8D)$  is equal to 0.02 m/s, and can be visualized using the multi-purpose video tools, whereas the reorientation dynamics of the 5CB under microfluidic confinement can be studied by polarized light microscope technique.

We believe that the precise handling of the LC microvolumes can be developed utilizing the interactions of both director and velocity fields with the radially directed temperature gradient. Hence, the possible pumping technique described above appears applicable to various experimental setups not involving mobile parts.

#### ACKNOWLEDGMENTS

The reported study was funded by RFBR (RU) and DFG (GE), Grant No. 20-52-12040.

- 
- [1] S. J. Woltman, G. D. Jay, and G. P. Crawford, *Nat. Mater.* **6**, 929 (2007).
  - [2] J. G. Cuennet, A. E. Vasdekis, L. De Sio, and D. Psalis, *Nat. Photon.* **5**, 234 (2011).
  - [3] A. P. H. J. Schenning, G. P. Crawford, and D. J. Broer, *Liquid Crystal Sensors* (CRC Press, Boca Raton, FL, 2018).
  - [4] T. M. Squires and S. R. Quake, *Rev. Mod. Phys.* **77**, 977 (2005).
  - [5] P. G. de Gennes and J. Prost, *The Physics of Liquid Crystals*, 2nd ed. (Oxford University Press, Oxford, 1995).
  - [6] A. V. Zakharov and A. A. Vakulenko, *J. Chem. Phys.* **127**, 084907 (2007).
  - [7] J. L. Ericksen, *Arch. Ration. Mech. Anal.* **4**, 231 (1960).
  - [8] F. M. Leslie, *Arch. Ration. Mech. Anal.* **28**, 265 (1968).
  - [9] L. D. Landau and E. M. Lifshitz, *Fluid Mechanics* (Pergamon, Oxford, 1987).
  - [10] M. C. Cross and P. C. Hohenberg, *Rev. Mod. Phys.* **65**, 851 (1993).
  - [11] R. V. Meyer, *Phys. Rev. Lett.* **22**, 918 (1969).
  - [12] J. N. Israelachvili, *Intermolecular and Surface Forces*, 2nd ed. (Academic Press, London, 1992).
  - [13] A. V. Zakharov, A. A. Vakulenko, and S. Romano, *J. Chem. Phys.* **132**, 094901 (2010).
  - [14] I. W. Stewart, *The Static and Dynamic Continuum Theory of Liquid Crystals* (Taylor & Francis, London, 2004).
  - [15] R. S. Akopyan and B. Ya. Zeldovich, *Sov. Phys. JETP* **60**, 953 (1984).
  - [16] R. S. Akopyan, R. B. Alaverdian, E. A. Santosyan, and Y. S. Chilingarian, *J. Appl. Phys.* **90**, 3371 (2001).
  - [17] M. Iwamoto and C. X. Wu, *The Physical Properties of Organic Monolayers* (World Scientific, Singapore, 2001).
  - [18] N. V. Madhusudana and R. B. Ratibha, *Mol. Cryst. Liq. Cryst.* **89**, 249 (1982).
  - [19] J. Jazdyn, S. Cherkas, G. Czechowski, A. Burczyk, and R. Dabrowski, *Liq. Cryst.* **26**, 437 (1999).
  - [20] A. G. Chmielewski, *Mol. Cryst. Liq. Cryst.* **132**, 339 (1986).
  - [21] P. Jamee, G. Pitsi, and J. Thoen, *Phys. Rev. E* **66**, 021707 (2002).
  - [22] M. Marinelli, A. K. Ghosh, and F. Mercuri, *Phys. Rev. E* **63**, 061713 (2001).
  - [23] S. R. de Groot and P. Masur, *Non-equilibrium Thermodynamics* (Dover, New York, 1984).
  - [24] I. S. Berezin and N. P. Zhidkov, *Computing Methods*, 4th ed. (Pergamon Press, Oxford, 1965).
  - [25] A. V. Zakharov, P. V. Maslennikov, and S. V. Pasechnik, *Phys. Rev. E* **103**, 012702 (2021).